Heat and Mass Transfer (2022) 58:887–901
https://doi.org/10.1007/s00231-021-03150-6

ORIGINAL ARTICLE

Investigation on spray cooling heat transfer performance with different nanoparticles and surfactants

Jun Bao[1] · Yu Wang[1] · Risto Kosonen[1,2] · Xinjie Xu[1] · Jinxiang Liu[1]

Received: 4 December 2020 / Accepted: 26 October 2021 / Published online: 2 November 2021
© The Author(s), under exclusive licence to Springer-Verlag GmbH Germany, part of Springer Nature 2021

Abstract

The spray cooling enhancement method has consistently been the focus area for research as a highly effective cooling method that can alter the properties of spray media by allowing the addition of different types of additives. In this study, an open spray cooling system was established for experimental purposes. Firstly, the effects of nozzles on the spray cooling characteristics were investigated through four kinds of nozzle experiments. Al_2O_3-H_2O, TiO_2-H_2O, ZrO_2-H_2O, and SiO_2-H_2O nanofluids were chosen as cooling substances based on the optimal nozzles, and the effects of the type and concentration of nanoparticles on cooling performance were studied. Based on the performance of the nanoparticles, sodium dodecyl benzenesulfonate(SDBS) was selected as the surfactant for Al_2O_3 and TiO_2 nanoparticles, while cetyltrimethyl ammonium bromide(CTAB) was selected as the surfactant for ZrO_2 and SiO_2 nanoparticles. The effects of surfactants with different concentrations on the heat transfer performance of nanofluids were studied. The results showed that when the mass fraction of SiO_2 nanoparticles was 0.2% and CTAB was 0.005%, an optimal cooling effect was achieved; which was 5.9% higher than that of water and 1.7% higher than that obtained without CTAB.

Nomenclature

h	Surface heat transfer coefficient, $W/m^2 \cdot K$
K_1	Thermocouple number i
q	Heat flux density at the heat source surface, W/m^2
Re	Reynolds number
T_1	Temperature measured by thermocouple K_1, °C
T_2	Temperature measured by thermocouple K_2, °C
T_3	Temperature measured by thermocouple K_3, °C
T_4	Temperature measured by thermocouple K_4, °C
T_{in}	Spray substance nozzle inlet temperature, °C
T_w	Temperature of the heat source surface, °C
We	Spray Weber number, $\rho_1 u_0^2 d_{32}/\sigma$
y_1	Distance from heat source surface to thermocouple K1, mm

Greek Letter

λ	Thermal conductivity of the copper heat source, W/m•K

✉ Yu Wang
yu-wang@njtech.edu.cn

1 College of Urban Construction, Nanjing Tech University, Nanjing 210009, China

2 Department of Mechanical Engineering, Aalto University, Sähkömiehentie 4, 02150 Espoo, Finland

1 Introduction

The increasing amount of heat generated by electronic equipment has led to a rapid growth in the demand for efficient cooling methods. Conventional liquid cooling solutions have been challenged when facing more complex application scenarios and higher heat fluxes. Microchannels, jet impingement, and spray cooling are three emerging and promising liquid cooling schemes that are favored by many scholars [1, 2]. Furthermore, spray cooling has a stronger heat dissipation capability than those of the traditional cooling methods. In addition, the temperature of the targeted surface is more uniform, and the thermal stress is lower than other emerging liquid cooling methods [3, 4]. Spray cooling has been gradually applied in various fields, such as data center chips [5, 6], spacecraft equipment [7–11], and other microelectronics cooling fields. In the scenarios with a high heat flux density, such as diode lasers and photovoltaic systems, spray cooling also has strong application potential and broad application prospects [12, 13].

Spray cooling is influenced by numerous factors, of which the medium characteristics are an important consideration. Different mediums have different heat transfer attributes. By using a single circular nozzle and controlling the mass flow rate of pure water and R-134a, Hsieh et al. [14] found that the subcooling degree of the R-134a used in the experiment was too low to have a significant impact on the cooling performance, while the highly subcooled water (55 and 60 °C) delayed the onset of saturated boiling. When the heat flux was 2×10^4 W/m^2 and *We* was 148, the heat transfer coefficient reached 6×10^3 W/m^2·°C. Mudawar et al. [15] evaluated the cooling performance, dielectric properties, safety, and material compatibility of different refrigerants. From their research, it was found that the evaluated performance of R-134a and HFE-7100 in Hydrofluorocarbons(HFCs) were relatively higher. Experiments showed that when HFE-7100 was used instead of R-134a to dissipate heat up to 200 W/cm^2, the surface temperature could be maintained below 125 °C. Therefore, using HFE-7100 as the coolant for spray cooling can meet the thermal management needs in hybrid vehicles. Liu et al. [16] used a mixture of water and ethanol as the working fluid and compared its performance with pure water as the working fluid. The experimental study demonstrated that the spray cooling performance of the mixture of water and ethanol was much better than that of pure water. The maximum heat transfer enhancement effect was achieved when the volume fraction of ethanol was 4%.

Researchers have found that adding an appropriate amount of surfactant to the water can reduce the surface tension of the medium, making droplets more likely to break, spread, and exchange heat with the surface [17], thus improving the heat transfer rate [18, 19].

Liu et al. [20] studied the enhancement effect of three surfactants on spray cooling performance under the inclined spray mode, including cetyltrimethyl ammonium bromide(CTAB), Tween 20, and sodium alpha-olefin Sulfonate(AOS). The experimental results showed that the optimum concentrations of CTAB, Tween 20, and AOS were 200, 30, and 300 ppm, respectively. However, bubbles produced by the high concentration of surfactant deteriorated the spray performance. Cheng et al. [21] studied the enhancement effect of high-alcohol surfactant on spray cooling in water. The experimental results showed that the addition of 200 ppm 1-octanol and 150 ppm 2-ethyl hexanol in water increased the heat transfer efficiency by 28% and 36% compared with that without additives, respectively. Ravikumar et al. [22] considered the cooling effect of adding a mixture of ionic surfactants, including sodium dodecyl sulfate (SDS) and CTAB, and a non-ionic surfactant (Tween 20) to water on a steel hot plate. It was found that during the atomization process in the nozzle, the droplets atomized from the cooling medium with a higher amount of surfactant were smaller, which indicates that the droplets have a smaller contact angle with the heated surface and higher wettability. Therefore, the surface cooling rates of the binary surfactant solutions used in the experiments, including SDS mixed with CTAB and CTAB mixed with Tween 20, were better than those of pure surfactant solutions. The best mixing volume ratio of SDS mixed with Tween 20 and CTAB mixed with Tween 20 was 25%:75%. Nayak et al. [23, 24] studied the cooling effect of three different nanofluids of Al_2O_3, TiO_2 and CuO on a hot steel plate with an initial temperature of 700 ℃ under jet impingement. The mass fractions were 0.1%, 0.3%, 0.5% and 0.7%, respectively. The study found that compared with deionized water and TiO_2 nanofluid, Al_2O_3 nanofluid has higher heat transfer characteristics due to its better dispersion effect. Zhang et al. [25] studied the effects of four high-alcohol surfactants on the heat transfer performance of spray cooling using water as a working fluid. The study found that when the concentration of 1-octanol was 0.3‰, the heat transfer performance reached the experimental maximum of 200.8 W/cm^2, followed by isooctanol concentration of 0.5‰, where the heat dissipation flux was 185 W/cm^2. The author also studied the effect of surfactant concentration on spray characteristics. The study found that a lower concentration of surfactant caused the surface tension of the medium to drop rapidly, but had little effect on the dynamic viscosity.

The thermal conductivity can be also enhanced by adding nanoscale metal or metal oxide particles to the cooling medium [26, 27]. In 1995, Choi [28] first advanced the concept of nanofluids, which drew the attention of numerous scholars to study the application of nanofluids for enhancing heat transfer in their own research field. For spray cooling, the heat transfer enhancement effect of using Al_2O_3 nanofluid as the cooling medium was investigated by Bansal and Pyrtle [29]. The results showed that the critical heat flux density of nanofluids was higher than that of water. Sun et al. [30] studied the heat transfer characteristics of deionized water, multiwalled carbon nanotube nanofluids, and Ag-multiwall carbon nanotube/water mixed nanofluids for mixed jet impingement and rotating jet impingement. The results showed that the heat transfer coefficient increased with the increase of particle mass fraction from 0.01%—0.05% in five kinds of hybrid nanofluids. In the traditional impinging jet and swirling impinging jet, compared with deionized water, the heat transfer coefficient of the 0.05% Ag-multiwall carbon nanotube/water hybrid nanofluid increased by 116.67% and 120.53%, respectively.

Some scholars have also found that under certain conditions, the addition of nanoparticles into the base solution will degrade the heat transfer capability [31–33]. Bellerová et al. [34] studied the spray cooling heat transfer performance of water-Al_2O_3 nanofluid. Under a constant mass flow rate, the heat transfer coefficient decreased by 45% as the volume fraction of the nanoparticles increased from 0 to 0.1645. It was concluded that during the investigation on nanofluids, a large number of nanoparticles would accumulate and form large-scale nanoclusters owing to their adsorption and nanoclusters would settle under the effect of gravity, which deteriorated the stability and heat transfer of the nanofluids.

As mentioned previously, both surfactants and nanomaterials can be applied to enhance spray cooling heat transfer. In addition, many studies have shown that the addition of an appropriate amount of surfactant during the preparation of nanofluids can improve the stability of nanofluids [35–37]. Therefore, to obtain optimal heat transfer performance, scholars have conducted experiments on the effect of the addition of surfactants in nanofluids on spray cooling performance.

Ravikumar et al. [38] conducted spray cooling experiments using nanofluids prepared with Al_2O_3 particles less than 13 nm in diameter and water. In general, compared with pure water (filtered drinking water), the cooling rate of Al_2O_3 nanofluids increased by 10.2% without a surfactant, and the optimal condition when adding a surfactant was water-Al_2O_3-Tween 20, which increased the cooling rate by 32.3% compared with pure water. Li et al. [39] discussed the effects of pH and sodium dodecyl benzenesulfonate(SDBS) on the thermal conductivity of copper nanoparticles. It was found that when the mass fraction of copper nanoparticles was 0.1%, the pH was 8.5–9.5, and when the mass fraction of SDBS was 0.02%, the thermal conductivity reached the maximum value, which was 10.7% higher than that of the base solution without nanoparticles. Wang et al. [40] studied the spray cooling heat transfer coefficient of Cu, CuO and Al_2O_3 nanofluids under different volume fractions and using Tween20 as dispersant. It was found that the thermal conductivity of CuO nanofluids increases with the increase of volume fraction. When the volume fraction was 0.5%, the thermal conductivity of CuO nanofluids was the largest, reaching 3.48 MW/cm^2. Surfactants reduced the contact angle of droplets and accelerated nucleate boiling. Chakraborty et al. [41] studied the effect of surfactants on the thermophysical properties, stability and heat transfer performance of Cu–Zn-Al LDH nanofluids. Two surfactants, SDS and Tween20, were selected in the study. The research results showed that SDS was better compatible with nanofluids and had better thermophysical properties. When the SDS concentration was 600 ppm, the heat exchange effect reached the best, which was 20.9% higher than when water was used for heat transfer. When the SDS concentration was 800 ppm, the stability of the nanofluid could be maintained for a longer time.At present, only aluminum additives have been sufficiently investigated for spray cooling, and research about other nanomaterials remains inadequate. In this paper, the effects of four different types of nanofluids, including Al_2O_3, TiO_2, SiO_2, and ZrO_2, on the cooling performance of spray cooling are evaluated for the first time. Furthermore, according to the obtained optimal nanoparticles, two kinds of surfactants, SDBS and CTAB, were used. The effect of the concentration of the surfactant on the cooling performance of nanofluids was studied, and the effects of different concentration ratios were compared. Considering that the potential application of our system is for the chip cooling in data center, the heat transfer is in the single-phase region. Therefore, the CHF was not considered in our experiment. The final section summarizes the main findings of this project and provides suggestions for the practical application and development of nanofluid spray cooling.

2 Experimental

2.1 Experimental rig

The spray cooling experimental system consisted of a spray medium supply system, a simulated heat source system, and a data acquisition system. Figure 1 shows a schematic of the

Fig. 1 Schematic of the spray cooling system

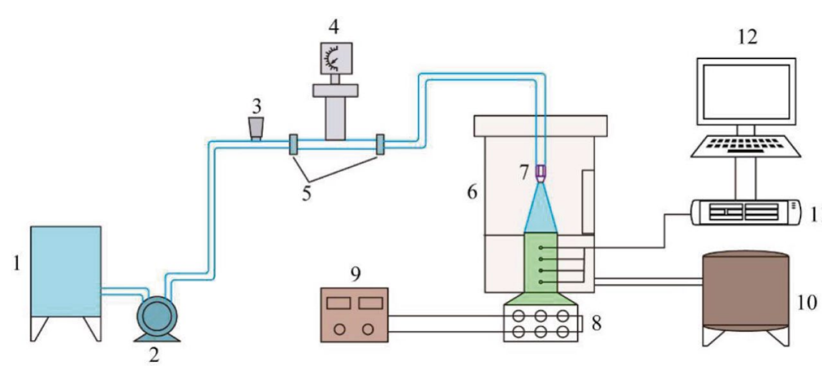

1. Liquid storage tank 2. Micro high-pressure pump 3. Flow regulating valve 4. Flowmeter 5. Flanges 6. Spray chamber 7. Spray nozzle 8. Heating pipe 9. Heating power regulator 10. Wastewater collection tank 11. Data acquisition instrument 12. Computer

experimental system. The spray medium supply system primarily includes a liquid storage tank, a micro high-pressure pump, a flow regulating valve, a flow meter, a medium conveying pipe, and a waste liquid collection tank. During the experiment, the cooling medium in the liquid storage tank was pumped by the micro high-pressure pump. The cooling medium flowed through the flow regulating valve and the flow meter and was sprayed onto the surface of the simulated heat source. After exchanging heat with the simulated heat source, the cooling medium flowed into the waste liquid collection tank for unified processing. A micro high-pressure pump from the Italian Fluid-o-Tech "compact" vane pump series was used, which can provide a maximum flow rate of 100 L/h. An LZ500 flow meter from Suzhou Xianchi Instrument Co., Ltd. was used with a range of 0 to 200 L/h and a maximum uncertainty of ± 5 L/h. Two narrow angle stainless steel nozzles (1/8G-SS1507 and 1/8G-SS1514) and two square stainless-steel nozzles (1/8G-SS3.6SQ and 1/8G-SS6SQ) from Spraying System Co. were selected as the experimental nozzles. The distance from the nozzle to the heating surface was 100 mm. In our previous study, it is found that with this height, the droplets from these four nozzles all can cover the heating surface [42].

A copper heating block was established, the upper surface of which was a circle with a diameter of 2.4 cm. Six electric heating rods with a power of 300 W were used as the input heating power. The maximum heating capacity of the simulated heat source was 1800 W. The instantaneous temperatures were collected by an Agilent 34972A data acquisition instrument.

To prepare the nanofluids, IKA company model RW20 digital overhead stirrers (shown in Fig. 2) and a KQ-50DE ultrasonic cleaner from Kunshan Ultrasonic Instrument Co., Ltd., (shown in Fig. 3) were used. The Al_2O_3, TiO_2 (rutile type), ZrO_2, and SiO_2 nanoparticles used in the experiments were provided by Shandong Taipeng New Material Co., Ltd., with a particle size of 75 nm. The surfactants used in this study, SDBS and CTAB, were provided by Tianjin Dingshengxin Chemical Co., Ltd., and Fuzhou Phygene Biological Co., Ltd., respectively. As shown in Fig. 4, four K-type thermocouples were arranged vertically on the copper column to measure the temperature at different positions. Calibration was performed before the measurements. The uncertainty of the equipment and specific parameters are shown in Tables 1 and 2.

2.2 Experimental procedures

For the experiments, the optimized nozzle was selected first. Then, a performance evaluation experiment with different nanoparticles and surfactants was carried out. As the steady state was reached, the measurement data was acquired for analysis.

Fig. 2 Overhead stirrer

2.2.1 Nozzle selection experimental procedure

In the experiment, nozzles with different types and pole sizes were selected. Under the conditions of constant flow and heat flux, spray cooling experiments were carried out with water as the cooling medium, and the cooling effects were compared. The nozzle which had the best cooling effect was selected as the nozzle for subsequent experiments. The nozzle optimization experimental procedure is as follows:

(1) Adjust the position of the nozzle height from the heating surface to 100 mm by rotating the thread above the spray chamber.

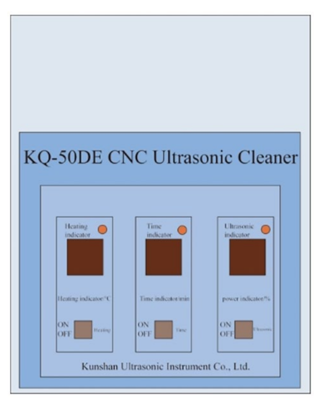

Fig. 3 Ultrasonic cleaner

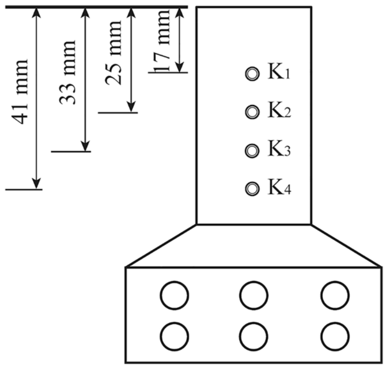

Fig. 4 Schematic of the vertical arrangement of the thermocouples

(2) Turn on the micro high-pressure pump and adjust the flow regulating valve to maintain a flow of 50 L/h.
(3) Turn on the heating tube and adjust the heating power regulator to maintain a surface heat flux density of 100 W/cm^2.
(4) Turn on the data acquisition instrument and computer to record the temperatures measured by the thermocouples.
(5) Record data when the steady state is achieved. Turn off the heating tube to stop heating.
(6) Keep the micro high-pressure pump working until the surface temperature of the heat source is reduced to the ambient temperature; then, turn off the micro high-pressure pump.
(7) Change the nozzle and repeat steps 3 to 6.

2.2.2 Nanoparticle concentration experimental procedure

The experiments concerning nanoparticle concentration were performed with the optimal nozzle selected through the procedure in Sect. 2.2.1. The effect of the mass fraction of nanoparticles in the nanofluid on the spray cooling performance was studied, and the optimal nanoparticle concentration was selected without adding a surfactant.

Table 2 Surfactant parameters

Surfactant type	Molecular formula	Relative molecular mass	Purity specifications
SDBS	$C_{18}H_{29}NaO_3S$	348.48	Analytical reagent
CTAB	$C_{19}H_{42}BrN$	364.45	Analytical reagent

Four nanomaterials (Al_2O_3, ZrO_2, SiO_2, and TiO_2) were selected for the experiment. The dispersion method was used to prepare the nanofluids. Considering the low mass fraction of the nanofluids used in this experiment and the short length of a single group of experiments, only mechanical stirring was used to disperse the nanoparticles. The procedure for preparing the nanofluids is as follows:

(1) Calculate the mass of water and nanomaterials needed to prepare the nanofluids according to the experimental scheme.
(2) According to the calculated mass, use the experimental balance to weigh the suitable nanomaterial, and use the graduate to measure the appropriate mass of water and place it in the beaker.
(3) Mix the nanomaterials with the water and stir at 500 rpm for 30 min to complete the preparation, as shown in Fig. 5.

After the cooling medium was prepared, the spray cooling process was performed as listed in Sect. 2.2.1.

2.2.3 Surfactant concentration experiments

According to the experiments in Sect. 2.2.2, the optimal mass fraction of nanomaterials for each nanoparticle was obtained, and the effect of the concentration of the added surfactant on the performance of spray-cooled nanofluids was studied. To further enhance the heat transfer performance, a surfactant was added in the cooling medium.

Table 1 Experiment equipment

Equipment name	Model	Manufacturer	Range	Accuracy
Thermocouples	K-type armored thermocouple	OMEGA Engineering Inc	0–1300 °C	± 0.8 °C
PT100 temperature sensor	WZP-291	Shanghai Jiutian Equipment Co., Ltd	-200–400 °C	± 0.15 °C
Micro high-pressure pump	PA104	Fluid-o-Tech	0–100 L/h	N/A
Data acquisition instrument	Agilent 34972A	Agilent Technologies Inc	N/A	N/A
Flow meter	LZ500	Suzhou Xianchi Co	0–200 L/h	± 5L/h
Ultrasonic cleaner	KQ-50DE	Kunshan Ultrasonic Instrument Co., Ltd	N/A	N/A
Overhead stirrer	RW20 digital	IKA	60–2000 rpm	±30 rpm
Spray nozzles	1/8G-SS1507, 1/8G-SS1514, 1/8G-SS3.6SQ, 1/8G-SS6SQ	Spraying System Co	N/A	N/A

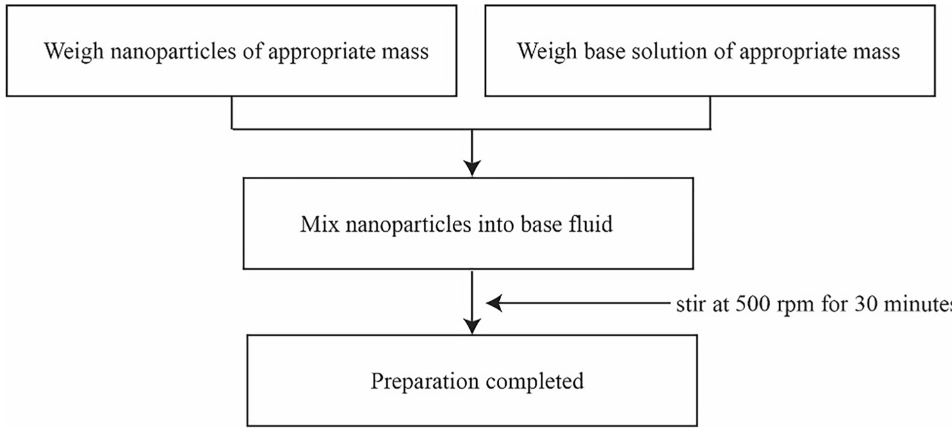

Fig. 5 Preparation of nanofluid without surfactant

For the Al_2O_3 [43] and TiO_2 nanoparticles [44], SDBS was used as the surfactant, and for SiO_2 and ZrO_2 nanoparticles, CTAB was used as the surfactant [45, 46]. The procedure is as follows:

(1) Calculate the mass of water, nanomaterials, and surfactants needed to prepare the nanofluid according to the experimental scheme.
(2) According to the calculated results, use an experimental balance to weigh the appropriate mass of water and surfactant.
(3) Mix water and surfactant in a beaker and use mechanical stirring to ensure that the surfactant is soluble in water.
(4) Add the nanoparticles to the mixture of water and surfactant, stir at 500 rpm for 30 min, and then use ultrasonic vibration for 1 h to prepare uniform Al_2O_3-SDBS-H_2O, TiO_2-SDBS-H_2O, ZrO_2-CTAB-H_2O, and SiO_2-CTAB-H_2O nanofluids, as shown in Fig. 6.

After the mixture of the nanomaterial and the surfactant was prepared, the spray cooling process was performed as listed in Sect. 2.2.1.

2.3 Data processing

As shown in Fig. 2, the distances between the K-type thermocouples K_1. K_2, K_3, and K_4 and the upper surface of the heat source were 17, 25, 33, and 41 mm, respectively. To set thermocouples in position, laser drilling was used on the thermocouple installation on the heat copper block. Because of the limitation of the processing technology, the uncertainty was $\pm$ 0.1 mm.

Using the temperature data from the four thermocouples collected by the data acquisition instrument, the

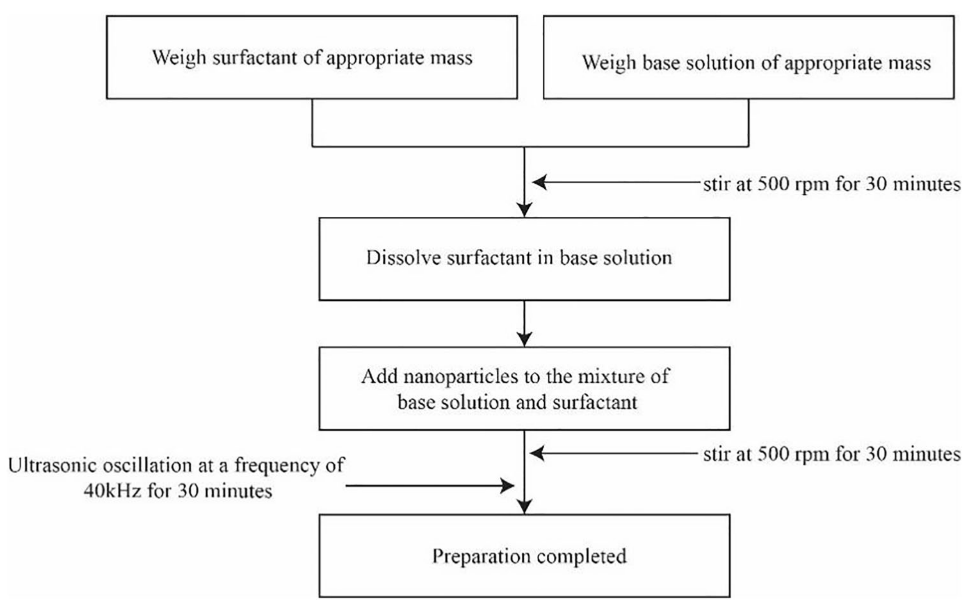

Fig. 6 Preparation of nanofluid with surfactant

temperature of the simulated heat source surface can be obtained by fitting to the one-dimensional Fourier heat conduction law:

$$q = \lambda \frac{\Delta T(y)}{\Delta y} \tag{1}$$

where q is the heat flux of the simulated heat source surface, λ represents the thermal conductivity of copper, and $\frac{\Delta T(y)}{\Delta y}$ is the slope of the temperature distribution, which can be obtained by fitting the temperature data from the four thermocouples.

The temperature of the surface of the heat source can be calculated from the following formula:

$$T_w = T_1 - \frac{\Delta T(y) y_1}{\Delta y} \tag{2}$$

where T_w represents the temperature of the surface of the heat source, T_1 is the temperature measured by thermocouple K_1, and y_1 represents the distance from the surface of the heat source to the thermocouple K_1.

The surface heat transfer coefficient can be obtained by the following formula.

$$h = \frac{q}{(T_w - T_{in})} \tag{3}$$

where h is the surface heat transfer coefficient between the cooling droplets and the heating surface, and T_{in} represents the nozzle inlet temperature of the cooling substance. Therefore, the temperature difference in Eq. (3) is the value between the surface temperature and the inlet temperature, which is represented by $T_w - T_{in}$. The nozzle inlet temperature was measured by a PT100 platinum resistance sensor.

Based on error transfer functions, on this experimental setup the uncertainty of heat flux, surface temperature and heat transfer coefficient can be expressed as follows:

$$\frac{\delta q}{q} = \sqrt{(\frac{\delta \lambda}{\lambda})^2 + (\frac{\delta T}{T})^2 + (\frac{\delta y}{y})^2} \tag{4}$$

$$\delta T_w = \sqrt{(\delta T_1)^2 + (\delta \Delta T)^2} \tag{5}$$

$$\frac{\delta h}{h} = \sqrt{(\frac{\delta q}{q})^2 + (\frac{\delta T_w}{T_w - T_{in}})^2 + (\frac{\delta T_{in}}{T_w - T_{in}})^2} \tag{6}$$

According to the error transfer functions in our previous study [10], the maximum uncertainties of the heat flux and heat transfer coefficients were ± 4.9% and ± 5.7% respectively.

3 Results and discussion

3.1 Comparison of the cooling performance of different nozzles

The nozzle diameter and shape are important factors that affect the spray cooling performance. As the diameter increases, the atomization performance of the nozzle is significantly changed. Meanwhile the shape of the nozzle also affects the distribution of droplets, thereby affecting the heat transfer performance. Therefore, in this section the nozzles for further experiments were selected from the square nozzles and narrow-angle nozzles with a diameter of 1.6 mm and 2.4 mm. In Fig. 7, the heat transfer performance of different nozzles is compared according to the heat transfer coefficient. Using the square nozzle, the heat transfer coefficient can reach a maximum of 1.24 $W/cm^2{\cdot}K$, while when using the narrow-angle nozzle, it can reach a maximum of 1.58 $W/cm^2{\cdot}K$. The cooling performance of the narrow-angle nozzles is better than that of the square type nozzles. As shown in Fig. 8, the droplets sprayed from the square type nozzles were distributed in square shapes that were larger than the heating surface, causing more than half of the droplets to be sprayed off of the heating surface. The flow of droplets that participated in the heat exchange was smaller, results in a worse heat transfer coefficient.

Because the spray angle of the narrow-angle nozzles was only 15 °, most of the droplets were concentrated on the heating surface, directly participating in the heat exchange with the heating surface. Therefore, the narrow-angle nozzles have a better heat transfer performance than the square nozzles.

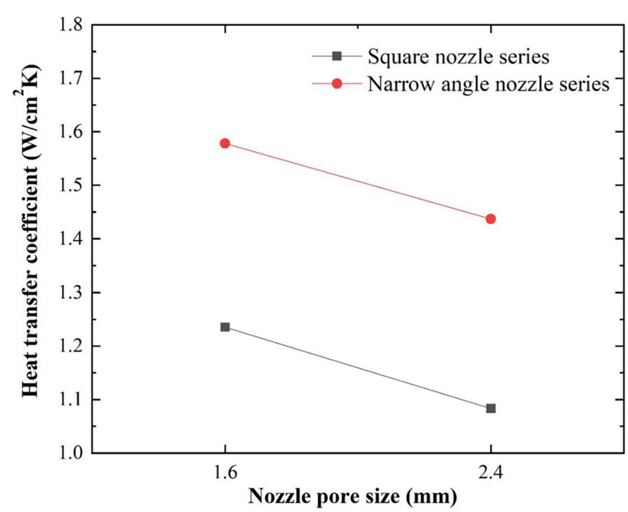

Fig. 7 Comparison of the cooling performance of different nozzles

Fig. 8 Droplet distribution of the square nozzle with pore size of 2.4 mm

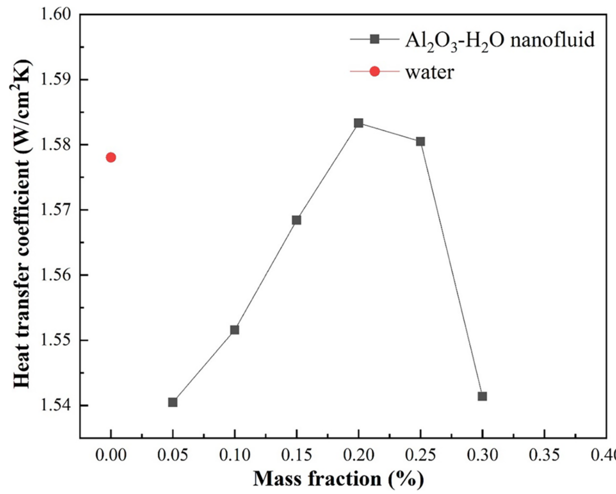

Fig. 9 Heat transfer coefficients for the spray cooling of Al_2O_3-H_2O nanofluids with different concentrations of nanoparticles

Regardless of the nozzle shape, as the nozzle diameter increased, the spray cooling heat transfer coefficient decreased. The reason is that under the condition of constant flow, a smaller nozzle diameter will cause the outlet pressure of the cooling medium to increase, thereby increasing the droplet ejection speed, accelerating the liquid film flow on the heating surface, and thus strengthen the heat exchange effect. Considering all the factors above, the narrow angle nozzle with pore size of 1.6 mm was applied in the following experiments.

3.2 Effects of nanofluid concentration without a surfactant on the heat transfer performance of spray cooling

3.2.1 Heat transfer performance of the Al_2O_3-H_2O nanofluid for spray cooling

Five groups of Al_2O_3 nanofluids with a mass fraction of 0.1 to 0.3% were prepared, and spray cooling experiments were carried out. The heat transfer coefficients of the Al_2O_3 nanofluids are shown in Fig. 9. In addition, the mass fraction of 0% in Fig. 9–15 and Fig. 17 means the experimental condition of using pure water. It can be seen from the figure that when the mass concentration of nanoparticles in the nanofluid increased from 0.1 to 0.2%, the heat transfer coefficient gradually increased. The maximum value of the heat transfer coefficient (1.58 $W/cm^2{\cdot}K$) was achieved when the mass fraction of nanoparticles in the Al_2O_3-H_2O nanofluid was 0.2%. For lower mass fractions, the interaction of the nanoparticles with disturbances in the heated surface liquid film and the irregular movement of nanoparticles can enhance heat transfer. As the mass fraction of the nanoparticles increased above 0.2%, the heat transfer coefficient showed a downward trend. When the mass fraction of nanoparticles in the Al_2O_3-H_2O nanofluid was 0.2–0.25%, the heat transfer effect was still superior to that of water, but the enhancement was limited because of the combined impact of the heating surface roughness and the deposition of nanoparticles on the surface, which created contact thermal resistance. At high concentrations, the particles accumulate on the heating surface, which isolates the cooling medium from the heat source and thus reduces the amount of heat exchanged. From the perspective of fluid flow on the heating surface, the increase in surface tension caused by a higher concentration of nanoparticles also impairs the fluid flow and the heat transfer. Specifically, the heat transfer coefficient of the Al_2O_3-H_2O nanofluid with the best mass fraction of 0.2% was only enhanced by 0.33% compared to water. The reason is that when using the narrow angle nozzle, the droplets are concentrated in a small area of the heating surface, which results in nonuniform heat transfer and has a negative impact on the heat transfer effect. At the same time, the continuously produced contact thermal resistance caused by the deposition of nanoparticles also has a negative effect.

3.2.2 Heat transfer performance of the TiO_2-H_2O nanofluid for spray cooling

The TiO_2-H_2O nanofluid spray cooling heat transfer coefficients for different concentrations of nanoparticles are shown in Fig. 10. It can be seen that when the mass fraction of nanoparticles in the TiO_2-H_2O nanofluid was 0.0125–0.025%, the heat transfer effect of the nanofluid was superior to that of water. In the first experimental point, the heat transfer effect of the nanofluid reached the optimal value, which corresponded with a mass fraction of 0.0125%. The reason is that the thermal conductivity of the TiO_2 particles

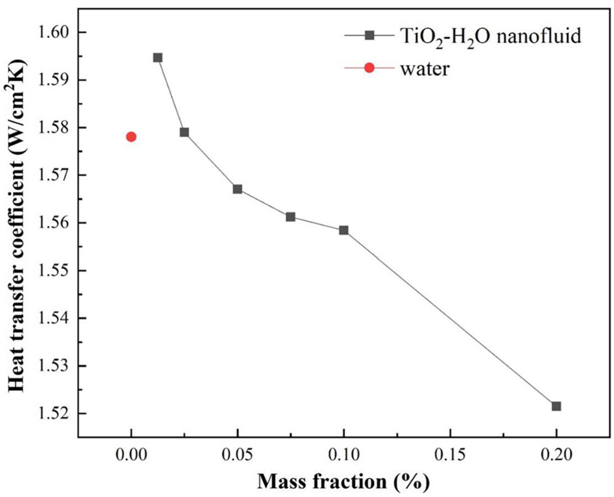

Fig. 10 Heat transfer coefficients for the spray cooling of TiO_2-H_2O nanofluids with different concentrations of nanoparticles

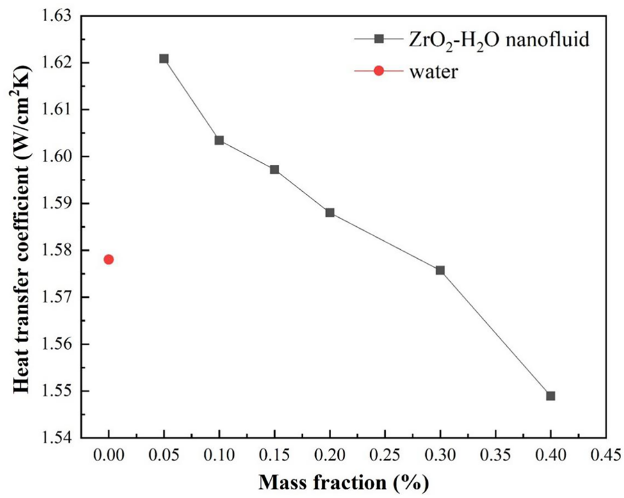

Fig. 11 Heat transfer coefficients for the spray cooling of ZrO_2-H_2O nanofluids with different concentrations of nanoparticles

(8.05 W/m·K) is greater than that of water (0.663 W/m·K) [47], and a small number of nanoparticles can disturb the liquid film. Because of these two factors, a low concentration of nanoparticles in the TiO_2-H_2O nanofluid can enhance the heat transfer effect of the fluid. As the mass fraction of nanoparticles in the TiO_2-H_2O nanofluid increased, the heat transfer coefficient gradually decreased. For mass fractions higher than 0.025%, the nanoparticles in the water had an increasingly significant role in deteriorating heat transfer. This phenomenon is also related to the thermal resistance caused by the deposited particles and the increasing surface tension of nanofluid. The TiO_2 nanoparticles used in the experiment were not surface modified, which allows them to easily absorb moisture from the air to form a liquid bridge. Under the static liquid bridge force, nanoparticles tend to agglomerate and form large nanoclusters, which are more detrimental than smaller nanoparticles to heat exchange with the heated surface. Therefore, even at a low concentration, that TiO_2-H_2O nanofluid has a poor heat transfer ability. In general, the heat transfer effects of Al_2O_3-H_2O and TiO_2-H_2O nanofluids share the same trend on the changes in the concentration of nanoparticles, and both show a phenomenon that the heat transfer effect decreases as the concentration of nanoparticles increases.

3.2.3 Heat transfer performance of the ZrO_2-H_2O nanofluid for spray cooling

Figure 11 shows the heat transfer coefficient of the heated surface when ZrO_2-H_2O nanofluids with different concentrations of nanofluids were applied. Similar to the TiO_2-H_2O nanofluids, the heat transfer coefficient reached the maximum value for the lowest mass fraction of ZrO_2 particles. As the mass fraction of nanoparticles increased, the heat transfer coefficient showed a downward trend. When the mass fraction of nanoparticles increased to 0.3%, the spray cooling performance was already worse than that of water, and the heat transfer coefficient continued to deteriorate as the mass fraction of nanoparticles increased further. The reason for the above phenomenon is the same as for the TiO_2-H_2O nanofluid.

3.2.4 Heat transfer performance of the SiO_2-H_2O nanofluid for spray cooling

With the SiO_2-H_2O nanofluid as the working fluid, the heat transfer phenomenon was similar to the Al_2O_3-H_2O nanofluid, as shown in Fig. 12. Heat transfer was enhanced as the concentration of SiO_2 nanoparticles increased within 0.1–0.2%, and the heat transfer coefficient reached 1.64 W/cm^2·K when the concentration was 0.2%, which is 4% higher than that of pure water. As the mass fraction of nanoparticles increased from 0.2 to 0.8%, the heat transfer coefficient decreased. The cooling performance was inferior to water when the mass fraction of SiO_2 nanoparticles increased to 0.6%.

At lower concentrations, a small number of nanoparticles can move and rotate randomly under the Brownian force, which can improve the heat transfer. The number of particles in the nanofluid increases as the concentration increases, resulting in a decrease in particle mobility. The increase in concentration also causes agglomeration of the nanoparticles and increases of kinematic viscosity of the nanofluids, resulting in an increase in the volume of droplets from the spray, which impairs heat transfer. The density of SiO_2 nanoparticles (2.2 g/cm^3) is smaller than that of Al_2O_3

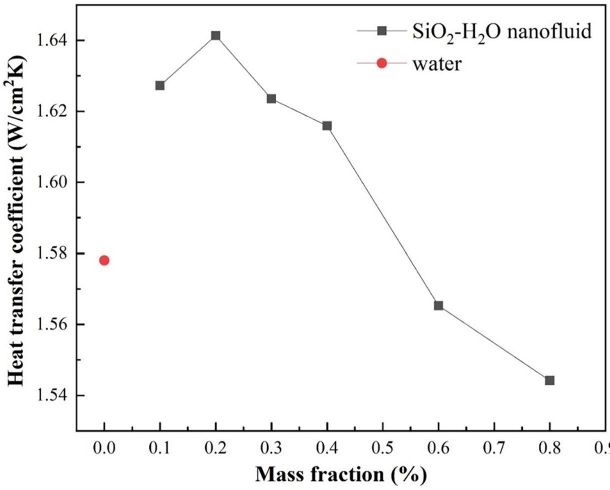

Fig. 12 Heat transfer coefficients for the spray cooling of SiO_2-H_2O nanofluids with different concentrations of nanoparticles

nanoparticles (3.9 g/cm^3). Therefore, at the same mass fraction, the SiO_2-H_2O nanofluid contains more SiO_2 nanoparticles, which makes the heat transfer coefficient of the SiO_2 nanofluid larger.

In summary, it was found that, compared with the water, nanoparticles could enhance the heat transfer coefficient at a low concentration. The reason is that at low concentrations, the Brownian motion of nanoparticles, which are constantly impacted by liquid molecules, can remove heat quickly [48]. During the spray process, the nanoparticles impacted the heated surface, which disturbed the liquid film and enhanced the heat transfer effect. By increasing the concentration of nanoparticles in the nanofluids, the heat transfer enhancement was reduced and even deteriorated at large concentrations. The main reasons are as follows:

(1) Because of the large number of particles in the high concentration nanofluids, the impact of the particles is reduced, and the possibility of collisions between nanoparticles and agglomerates is greatly increased, resulting in a weakening of the Brownian motion of the particles and the capacity to transfer energy.
(2) The increase in the concentration of nanoparticles in the nanofluids leads to an increase in the liquid viscosity and surface tension, which directly affects the nozzle atomization effect.
(3) Because of the influence of heating surface roughness, nanoparticles will remain on the heating surface after contacting with the surface, and even sinter onto the surface at high temperatures, creating surface thermal resistance that isolates the cooling medium from the heating surface, and the increase in the mass fraction of nanoparticles in the nanofluid undoubtedly aggravates this phenomenon.

Therefore, adding only nanoparticles into water does not sufficiently enhance the heat transfer performance. Other additives should be added into the cooling medium to ensure adequate Brownian motion of the particles and reduce the thermal resistance.

3.3 Effect of adding surfactant on the heat transfer performance of nanofluid spray cooling

Surfactants can be added into the nanofluid to achieve a uniform particle distribution. To better enhance the spray cooling of the nanofluid, two typical surfactants, SDBS and CTAB, were selected according to the types of nanoparticles. SDBS was used to disperse the Al_2O_3 and TiO_2 nanoparticles [43], while CTAB was used to disperse the ZrO_2 and SiO_2 nanoparticles. The mass fractions of the four type of nanoparticles in the above experiments corresponding to the highest heat transfer coefficients were selected for subsequent experiments.

3.3.1 Effects of the SDBS surfactant on Al_2O_3-H_2O and TiO_2-H_2O nanofluids

Figure 13 shows the heat transfer coefficients of the Al_2O_3-SDBS-H_2O nanofluids with different mass fractions of SDBS. When the mixing ratio of SDBS and Al_2O_3 nanoparticles was 1:20, and the mass fraction of SDBS was 0.01% [49], the heat transfer coefficient of nanofluid reached 1.61 W/cm^2·K, which is slightly better than that of the nanofluid without SDBS and pure water. When the concentration of SDBS increased to 0.02%, the mixing ratio of SDBS and Al_2O_3 nanoparticles was 1:10, and the heat transfer performance became worse than the nanofluid without the surfactant. The reason is that when the surfactant concentration is relatively low, the surfactant adsorbs onto the nanoparticles, reducing the surface tension of the particles. Therefore, particle agglomeration can be avoided. The steady small particle field can improve the heat transfer ability. When the mass fraction of the surfactant is high, the viscosity of the base solution increases, and at the same time, too many active agents are adsorbed around the nanoparticles, which may reduce the Brownian motion of the particles and also enlarge the volume of the nanoparticles.

Figure 14 shows the heat transfer coefficients of the TiO_2-SDBS-H_2O nanofluids with different mass fractions of SDBS. When the mixing ratio of the surfactant and nanoparticles was 1:10 and the mass fraction of SDBS was 0.00125%, the heat transfer coefficient reached a maximum of 1.59 W/cm^2·K, which is slightly lower than the cooling performance without the surfactant. As the mixing ratio increased from 1:10 to 1:1, the heat transfer performance decreased. When the mixing ratio of surfactant and TiO_2 nanoparticles reached 1:2, and the mass fraction of SDBS

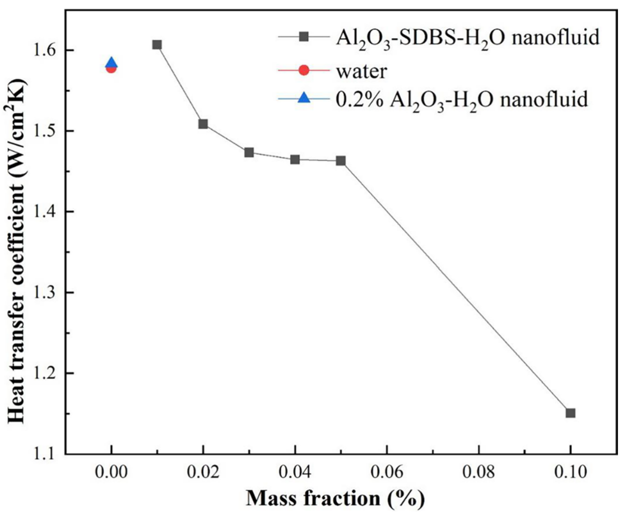

Fig. 13 Heat transfer coefficients for the spray cooling of Al_2O_3-SDBS-H_2O nanofluids with different concentrations of SDBS

was 0.00625%, the cooling performance of TiO_2-SDBS-H_2O was worse than that when using water as a cooling medium. As the mass fraction of surfactant further increased to 0.05%, the heat transfer performance declined rapidly. The cooling performance of the mixed media with different concentrations of surfactant in TiO_2 nanofluids did not reach the performance of that without surfactant, which indicates that the heat transfer could not be enhanced.

Because of the serious agglomeration of TiO_2, the addition of SDBS in TiO_2-H_2O with ultrasonic vibration failed to have a good dispersion effect on the micro-clusters in the nanofluid and failed to have a positive effect on the heat transfer. At the same time, it was found that after adding the SDBS surfactant and using mechanical agitation and ultrasonic vibration, TiO_2 nanoparticles still showed significant agglomeration.

3.3.2 Effects of the CTAB surfactant on ZrO_2-H_2O and SiO_2-H_2O nanofluids

Figure 15 illustrates the heat transfer coefficients of the ZrO_2-CTAB-H_2O nanofluids with different mass fractions of CTAB. It can be seen from the figure that when the mass fraction ratio of CTAB and ZrO_2 nanoparticles increased from 1:40 to 1:30, the heat transfer coefficient of the nanofluid increased slightly and reached the maximum of 1.65 $W/cm^2{\cdot}K$. As the CTAB concentration increased further, the heat transfer coefficient decreased. When the mass fraction of CTAB was 0.002%, the heat transfer coefficient of the mixed fluid was smaller than that without the surfactant. When the mass fraction of CTAB was 0.01%, the ZrO_2-CTAB-H_2O nanofluid no longer had an advantage over pure water cooling. The reason is that a low concentration of the surfactant can prevent the agglomeration of particles. In addition, a small amount of bubbles will be produced when a nanofluid with a low concentration of surfactant contacts the heating surface, which will disturb the liquid film on the heating surface. With a high surfactant concentration in the nanofluid, a large amount of foam will be generated, which will hinder the heat transfer between the droplet and the heated surface. Therefore, the higher the concentration, the worse the heat transfer effect. Figure 16 shows the spray chamber for different CTAB concentrations in the ZrO_2-CTAB-H_2O nanofluid after the heat transfer reached steady state.

Figure 17 shows the heat transfer coefficient of SiO_2-CTAB-H_2O nanofluids with different mass fractions

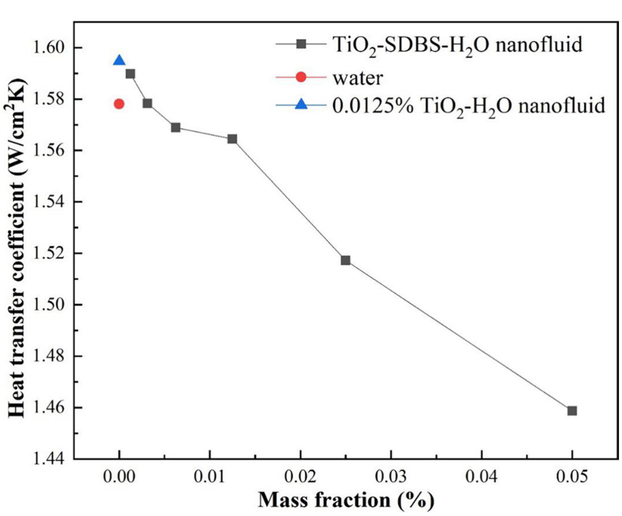

Fig. 14 Heat transfer coefficients for the spray cooling of TiO_2-SDBS-H_2O nanofluids with different concentrations of SDBS

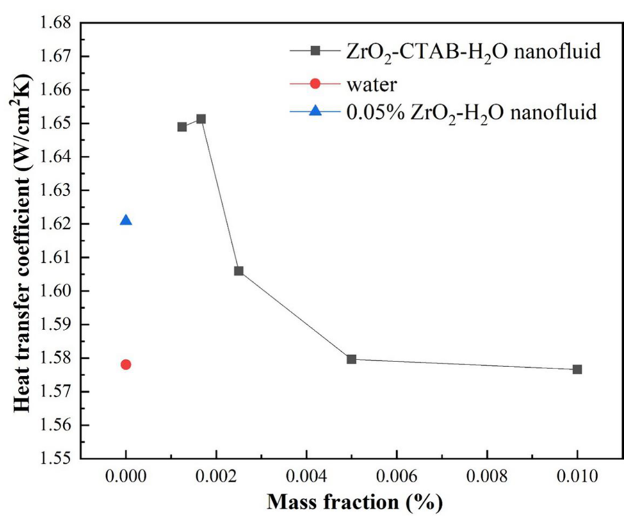

Fig. 15 Heat transfer coefficients for the spray cooling of ZrO_2-CTAB-H_2O nanofluids with different concentrations of CTAB

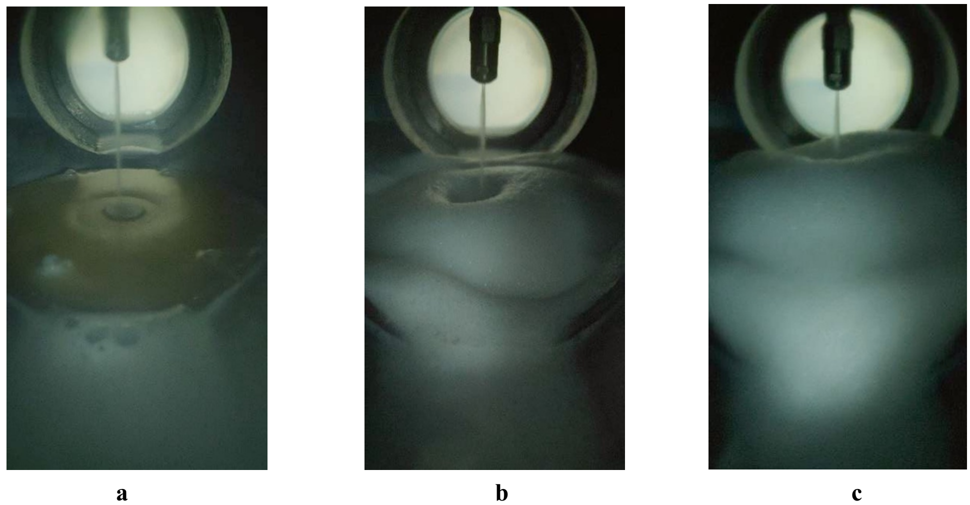

Fig. 16 Foaming of ZrO_2-H_2O-CTAB nanofluids in the spray chamber

a. Mass fraction ratio of ZrO_2 nanoparticles to CTAB is 40:1
b. Mass fraction ratio of ZrO_2 nanoparticles to CTAB is 20:1
c. Mass fraction ratio of ZrO_2 nanoparticles to CTAB is 5:1

of CTAB. Firstly, the heat transfer coefficient of the nanofluids increased as the CTAB concentration increased. When the mass fraction ratio of SiO_2 to CTAB was 40:1, the heat transfer capacity of the SiO_2-CTAB-H_2O nanofluid reached the maximum value of 1.67 W/cm^2·K, which is 5.9% higher than that of using water as the cooling medium and 1.7% higher than that of the SiO_2 nanofluid without the surfactant. The reason is that a small amount of surfactant reduces the agglomeration of the nanoparticles, while a small amount of foam increases the movement of nanoparticles. When the mass fraction of CTAB reached 0.1%, the heat transfer effect was worse than that without the surfactant. The reason is that the foam produced by a high concentration of surfactant hinders the contact between the droplets and the surface.

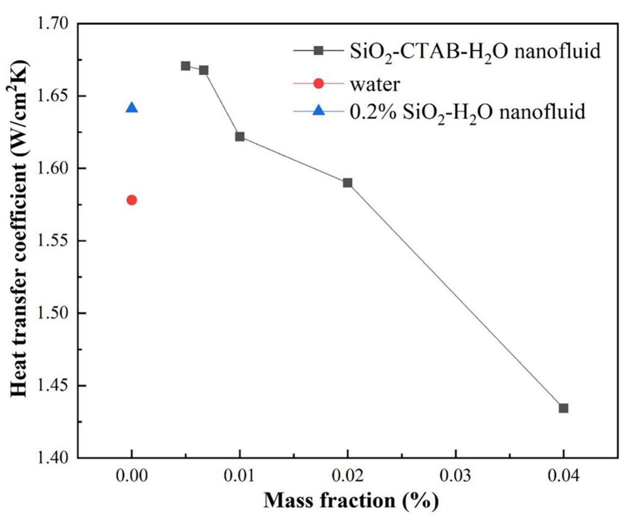

Fig. 17 Heat transfer coefficients for the spray cooling of SiO_2-CTAB-H_2O nanofluids with different concentrations of CTAB

According to the experimental observations shown in Fig. 18, the foaming property of the CTAB surfactant will cause the cooling medium containing the surfactant to produce bubbles when it impacts the cooled surface. The subsequent spraying will cause the bubbles to break on the impact surface, and at the same time, new bubbles will be produced. The generation and rupture of bubbles can enhance the heat transfer by disturbing the liquid film on the heating surface. However, if the surfactant concentration is high, the rapid generation of a large amount of foam will isolate the heat transfer between the droplets and the heated surface. Therefore, a high amount of the CTAB surfactant will impair the heat transfer.

In summary, only small amounts of the SDBS and CTAB surfactants can promote the heat transfer slightly. If the mass fraction is high, the property changes in the nanofluids will cause the deterioration of the heat transfer in spray cooling.

3.4 Limitations

The selection of nozzles, the optimization of nanoparticle types, and the proportion of nanoparticle and surfactant mass fraction are considered in Sect. 3.3 for nanofluid spray cooling experiments. However, there are still limitations in the investigation that require further follow-up study, including: (1) how to maintain the stability of the nanofluid to ensure the heat transfer performance of the nanofluid with the surfactant; (2) how to reduce the large amount of foam aggregation generated by the surfactant; and (3) after adding the nanoparticles and surfactants, how the increased cooling

Fig. 18 Foaming of SiO_2-CTAB-H_2O nanofluids in the spray chamber

a b c

a. Mass fraction ratio of SiO_2 nanoparticles to CTAB is 40:1

b. Mass fraction ratio of SiO_2 nanoparticles to CTAB is 20:1

c. Mass fraction ratio of SiO_2 nanoparticles to CTAB is 5:1

medium kinematic viscosity affects the pumping capacity of the whole cooling cycle.

In the actual application process of spray cooling with nanofluids, in areas such as data centers and spacecraft, the following problems must also be addressed: (1) After the start-up of the system, the mixing state of the fluid and water should be confirmed. (2) The effects of the increased kinematic viscosity of the nanofluids and the corrosion of pipelines on the pumping performance of the liquid cycle should be considered. (3) Whether the increased cost of using nanofluids is cost-effective compared to the heat transfer benefits obtained should be taken into consideration.

4 Conclusions

In this paper, the nozzle with the best cooling effect under a heating power of 100 W/cm^2, cooling medium of pure water, and medium flow of 50 L/h was selected through experiments, and the nozzle performances were compared. The cooling performance of four nanofluids (Al_2O_3-H_2O, TiO_2-H_2O, ZrO_2-H_2O, and SiO_2-H_2O) as the cooling media was studied. The effect of the concentration of two surfactants on the heat transfer performance of nanofluids was also studied, which was SDBS for Al_2O_3-H_2O and TiO_2-H_2O nanofluids and CTAB for ZrO_2-H_2O and SiO_2-H_2O nanofluids.

The conclusions are as follows:

(1) Compared with the square nozzles, the droplets sprayed by the narrow angle nozzles are more concentrated on the surface of the heat sink and directly participate in the heat exchange. Therefore, the spray cooling performance of the square nozzle is inferior to that of the narrow-angle nozzle. Under constant flow condition, smaller nozzle diameter can have higher droplet velocity and enhance heat transfer effect. For both nozzle types, the heat transfer capacity of the spray decreases with increasing nozzle diameter.

(2) The Brownian motion of low-concentration nanoparticles can better disturb the liquid film and enhance the heat transfer effect. The agglomeration of particles in the high-concentration nanofluid and the increase of fluid viscosity and surface tension will cause the deterioration of the nozzle atomization effect and lead to the decrease of heat exchange performance. When the mass fraction of the nanoparticles is low, a small amount of nanoparticles will enhance the heat transfer performance compared with pure water, while a larger concentration will cause the heat transfer effect to degrade.

(3) Al_2O_3 and TiO_2 nanoparticles absorb moisture to form static liquid bridges large agglomerations. Therefore, the effect of SDBS dispersion is not obvious, and the strengthening effect of the SDBS surfactant on the heat transfer performance of Al_2O_3-H_2O and TiO_2-H_2O nanofluids is not significant. At low concentrations, the CTAB surfactant provides a modest enhancement of the heat transfer effect for SiO_2-H_2O and ZrO_2-H_2O nanofluids.

(4) The lower concentration of CTAB has an obvious effect on the dispersion of nanoparticles, and the disturbance of the liquid film by a small amount of foam generated during the experiment also enhances the heat transfer. The maximum heat transfer coefficient in all the experi-

mental results are achieved when the mass fraction of SiO_2 nanoparticles is 0.2% and the CTAB concentration is 0.005%. In this condition, the heat transfer coefficient is increased by 5.9% compared to pure water.

Funding This work is supported by the National Natural Science Foundation of China (Grant No. 51806096), China Postdoctoral Science Foundation (No. 2019M661812), Postgraduate Research & Practice Innovation Program of Jiangsu Province (Grant No. SJCX20_0332), Natural Science Foundation of the Jiangsu Higher Education Institutions of China (Grant No. 18KJB560007), and the Research Fund of Key Laboratory of Aircraft Environment Control and Life Support, MIIT, Nanjing University of Aeronautics and Astronautics(Grant No. KLAECLS-E-201902).

Data availability The datasets used or analysed during the current study are available from the corresponding author on reasonable request.

Declarations

Conflicts of interest On behalf of all authors, the corresponding author states that there is no conflict of interest.

References

1. Mudawar I (2001) Assessment of high-heat-flux thermal management schemes. IEEE Trans Compon Packag Technol 24:122–141
2. Wang J-X, Guo W, Xiong K, Wang S-N (2020) Review of aerospace-oriented spray cooling technology, Progress in Aerospace Sciences 116:100635
3. Kandlikar SG, Bapat AV (2007) Evaluation of jet impingement, spray and microchannel chip cooling options for high heat flux removal. Heat Transfer Eng 28:911–923
4. Bostanci H, Van Ee D, Saarloos BA, Rini DP, Chow LC (2012) Thermal management of power inverter modules at high fluxes via two-phase spray cooling. IEEE Transact Components Packaging Manufacturing Technol 2:1480–1485
5. Pautsch G (1999) Thermal management of multichip modules with evaporative spray cooling, Proc. Pacific Rim/ASME International and Intersociety Electronic and Photonic Packaging Conf. 1453–1461
6. Pautsch G (2021) An overview on the system packaging of the CRAY SV2 supercomputer, Proceedings of IPACK 2001617–624
7. Kim J (2007) Spray cooling heat transfer: The state of the art. Int J Heat Fluid Flow 28:753–767
8. Shedd TA (2007) Next generation spray cooling: high heat flux management in compact spaces. Heat Transfer Eng 28:87–92
9. Silk EA, Golliher EL, Selvam RP (2008) Spray cooling heat transfer: technology overview and assessment of future challenges for micro-gravity application. Energy Convers Manage 49:453–468
10. Wang Y, Zhou N, Yang Z, Jiang Y (2016) Experimental investigation of aircraft spray cooling system with different heating surfaces and different additives. Appl Therm Eng 103:510–521
11. Wang J-X, Li Y-Z, Li J-X, Li C, Zhang Y, Ning X-W (2019) A gas-atomized spray cooling system integrated with an ejector loop: Ejector modeling and thermal performance analysis. Energy Convers Manage 180:106–118
12. Cheng W-L, Zhang W-W, Chen H, Hu L (2016) Spray cooling and flash evaporation cooling: the current development and application. Renew Sustain Energy Rev 55:614–628
13. Ge M, Wang Z, Liu L, Zhao J, Zhao Y (2018) Performance analysis of a solar thermoelectric generation (STEG) system with spray cooling. Energy Convers Manage 177:661–670
14. Hsieh S-S, Fan T-C, Tsai H-H (2004) Spray cooling characteristics of water and R-134a. Part I: nucleate boiling, International Journal of Heat and Mass Transfer 47:5703–5712
15. Mudawar I, Bharathan D, Kelly K, Narumanchi S (2009) Two-phase spray cooling of hybrid vehicle electronics. IEEE Trans Compon Packag Technol 32:501–512
16. Liu H, Cai C, Yin H, Luo J, Jia M, Gao J (2018) Experimental investigation on heat transfer of spray cooling with the mixture of ethanol and water. Int J Therm Sci 133:62–68
17. Lee S, Choi SUS (1996) Application of metallic nanoparticle suspensions in advanced cooling systems, Argonne National Lab., IL (United States)
18. Cheng L, Mewes D, Luke A (2007) Boiling phenomena with surfactants and polymeric additives: a state-of-the-art review. Int J Heat Mass Transf 50:2744–2771
19. Wasekar VM (2009) Heat transfer in nucleate pool boiling of aqueous SDS and triton X-100 solutions. Heat Mass Transf 45:1409–1414
20. Liu N, Zhan T-J, Zhang Y-W, Yin X-M, Zhang L-X (2019) Experimental investigation of comprehensive effects of surfactant and inclined mode on spray cooling heat transfer. Int J Therm Sci 136:457–466
21. Cheng W, Xie B, Han F, Chen H (2013) An experimental investigation of heat transfer enhancement by addition of high-alcohol surfactant (HAS) and dissolving salt additive (DSA) in spray cooling. Exp Thermal Fluid Sci 45:198–202
22. Ravikumar SV, Jha JM, Sarkar I, Pal SK, Chakraborty S (2014) Mixed-surfactant additives for enhancement of air-atomized spray cooling of a hot steel plate. Exp Thermal Fluid Sci 55:210–220
23. Nayak SK, Mishra PC, Parashar S (2016) Enhancement of heat transfer by water–Al2O3 and water–TiO2 nanofluids jet impingement in cooling hot steel surface. J Exp Nanosci 11:1253–1273
24. Nayak SK, Mishra PC (2019) Enhanced Heat Transfer from Hot Surface by Nanofluid based Ultrafast Cooling: An Experimental Investigation, Journal of Enhanced Heat Transfer 26
25. Zhang W-W, Li Y-Y, Long W-J, Cheng W-L (2018) Enhancement mechanism of high alcohol surfactant on spray cooling: Experimental study. Int J Heat Mass Transf 126:363–376
26. Nguyen CT, Roy G, Gauthier C, Galanis N (2007) Heat transfer enhancement using Al2O3–water nanofluid for an electronic liquid cooling system. Appl Therm Eng 27:1501–1506
27. Vafaei S, Borca-Tasciuc T (2014) Role of nanoparticles on nanofluid boiling phenomenon: Nanoparticle deposition. Chem Eng Res Des 92:842–856
28. Choi SU, Eastman JA (1995) Enhancing thermal conductivity of fluids with nanoparticles, Argonne National Lab., IL (United States)
29. Bansal A Pyrtle F (2007) Alumina nanofluid for spray cooling enhancement ASME/JSME 2007 Thermal Engineering Heat Transfer Summer Conference collocated with the ASME 2007 InterPACK Conference Am Soc Mech Eng Digital Collect 797 803
30. Sun B, Zhang Y, Yang D, Li H (2019) Experimental study on heat transfer characteristics of hybrid nanofluid impinging jets. Appl Therm Eng 151:556–566
31. Bang IC, Chang SH (2005) Boiling heat transfer performance and phenomena of Al2O3–water nano-fluids from a plain surface in a pool. Int J Heat Mass Transf 48:2407–2419
32. Liu Z-H, Qiu Y-H (2007) Boiling heat transfer characteristics of nanofluids jet impingement on a plate surface. Heat Mass Transf 43:699–706
33. Duursma G, Sefiane K, Kennedy A (2009) Experimental studies of nanofluid droplets in spray cooling. Heat Transfer Eng 30:1108–1120

34. Bellerová H, Tseng AA, Pohanka M, Raudensky M (2012) Spray cooling by solid jet nozzles using alumina/water nanofluids. Int J Therm Sci 62:127–137
35. Hwang Y, Lee J-K, Lee J-K, Jeong Y-M, Cheong S-I, Ahn Y-C, Kim SH (2008) Production and dispersion stability of nanoparticles in nanofluids. Powder Technol 186:145–153
36. Xia G, Jiang H, Liu R, Zhai Y (2014) Effects of surfactant on the stability and thermal conductivity of Al2O3/de-ionized water nanofluids. Int J Therm Sci 84:118–124
37. Zin V, Agresti F, Barison S, Colla L, Gondolini A, Fabrizio M (2013) The synthesis and effect of copper nanoparticles on the tribological properties of lubricant oils. IEEE Trans Nanotechnol 12:751–759
38. Ravikumar SV, Haldar K, Jha JM, Chakraborty S, Sarkar I, Pal SK, Chakraborty S (2015) Heat transfer enhancement using air-atomized spray cooling with water–Al2O3 nanofluid. Int J Therm Sci 96:85–93
39. Li X, Zhu D, Wang X, Wang N, Gao J, Li H (2008) Thermal conductivity enhancement dependent pH and chemical surfactant for Cu-H2O nanofluids. Thermochim Acta 469:98–103
40. Wang B, Liu Z, Zhang B, Xia Y, Wang Z, Wang G (2020) Effect of nanoparticle type and surfactant on heat transfer enhancement in spray cooling. J Therm Sci 29:708–717
41. Chakraborty S, Sengupta I, Sarkar I, Pal SK, Chakraborty S (2019) Effect of surfactant on thermo-physical properties and spray cooling heat transfer performance of Cu-Zn-Al LDH nanofluid. Appl Clay Sci 168:43–55
42. Bao J, Wang Y, Xu X, Niu X, Liu J, Qiu L (2019) Analysis on the influences of atomization characteristics on heat transfer characteristics of spray cooling. Sustain Cities Soc 51:101799
43. Zhu D, Li X, Wang N, Wang X, Gao J, Li H (2009) Dispersion behavior and thermal conductivity characteristics of Al2O3–H2O nanofluids. Curr Appl Phys 9:131–139
44. Duangthongsuk W, Wongwises S (2010) An experimental study on the heat transfer performance and pressure drop of TiO2-water nanofluids flowing under a turbulent flow regime. Int J Heat Mass Transf 53:334–344
45. Wang W, Gu B, Liang L (2005) Effect of surfactants on the formation, morphology, and surface property of synthesized SiO2 nanoparticles. J Dispersion Sci Technol 25:593–601
46. Esmaeilzadeh P, Fakhroueian Z, Bahramian A, Arya S (2013) Influence of ZrO2 Nanoparticles including SDS and CTAB Surfactants Assembly on the Interfacial Properties of Liquid-Liquid, Liquid-Air and Liquid-Solid Surface Layers, Journal of Nano Research, Trans Tech Publ 15–21
47. Tseng AA, Bellerová H, Pohanka M, Raudensky M (2014) Effects of titania nanoparticles on heat transfer performance of spray cooling with full cone nozzle. Appl Therm Eng 62:20–27
48. Jang SP, Choi SU (2004) Role of Brownian motion in the enhanced thermal conductivity of nanofluids. Appl Phys Lett 84:4316–4318
49. Wang X-J, Zhu D-S (2009) Investigation of pH and SDBS on enhancement of thermal conductivity in nanofluids. Chem Phys Lett 470:107–111

Publisher's Note Springer Nature remains neutral with regard to jurisdictional claims in published maps and institutional affiliations.